Nature Environment and Pollution Technology
An International Quarterly Scientific Journal

p-ISSN: 0972-6268
(Print copies up to 2016)
e-ISSN: 2395-3454

Vol. 22 | No. 1 | pp. 303-309 | 2023

Original Research Paper

https://doi.org/10.46488/NEPT.2023.v22i01.030

Open Access Journal

Study of Some Stability Parameters in the Atmosphere of Oil Al-Dura Refinery, Southeast Baghdad

Farant H. S. Lagenean*, Salwa S. Naif* and Monim H. Al-Jiboori*†

*Atmospheric Sciences Department, College of Science, Mustansiriyah University, Baghdad, Iraq

†Corresponding author: Monim H. Al-Jiboori; mhaljiboori@gmail.com

Nat. Env. & Poll. Tech.
Website: www.neptjournal.com

Received: 09-06-2022
Revised: 15-07-2022
Accepted: 18-07-2022

Key Words:
Atmospheric stability
Al-Dura refinery
Bulk Richardson number
Gradient Richardson number
Monin-Obukhov length

ABSTRACT

Wind and temperature measurements at an oil refinery site located southeast of Baghdad city at two levels, 15 and 30 m, are presented. Three schemes are used to determine different stability classifications: Monin-Obukhov length, gradient, and bulk Richardson numbers. Meanwhile, vertical changes in air temperature and wind shear are also computed. There were lapse rate and inversion cases during the nights and days while favorable wind shear was dominant. The variation of stability in each scheme is large, covering the entire range of stability for a given class. The results of stability schemes are compared to each other. The results show that the schemes based on gradient and bulk Richardson numbers reasonably compare them.

INTRODUCTION

The study of atmospheric stability classification is required to quantify the dispersion capability of ambient atmosphere in the air quality models for concentration prediction. Also, it is of prime concern for estimating the heat and momentum fluxes in the surface boundary layer (Anto et al. 1980, Al-Jiboori et al. 2001). This study, in terms of its degree and intensity, has the most important role in the transport and behavior of air pollutants (Lazaridis 2011). Furthermore, it represents a primary parameter in the expressions describing wind speed and temperature profiles (Al-Jiboori 2010, Newman & Klein 2014, Rodrigo et al. 2015). It can be defined as the atmospheric tendency to reduce or intensify the vigor of vertical motion or to suppress or augment existing turbulence (Seinfeld & Pandis 1998). Therefore it is related to vertical changes in air temperature and wind speed. In general, there are three states of atmospheric stability at low altitudes (i.e., less than 100 m): unstable, neutral, and stable.

There were different methods to determine the stability and instability with varying degrees of complexity. There are more than seven classification schemes, such as Pasqill-Gifford-Turner, the horizontal wind direction standard deviation, temperature gradient, gradient Richardson number, bulk Richardson number, Monin-Obukhov (M-O) length, and wind speed ratio. Most of these methods are based on the relative importance of convective and mechanical production in atmospheric motions. The difference between such methods is due to the use of various parameters for this production. Atmospheric stability is divided into seven categories starting from A to G, designated as: A (highly unstable or convective), B (moderately unstable), C (slightly unstable), D (neutral), E moderately stable, and F (extremely stable). Stability G is added to represent low wind night stable conditions as in urban areas (Mohan and Siddiqui, 1998). In this paper, these stability parameters will be determined, and their results will be compared through the frequency percentage.

MATERIALS AND METHODS

Atmospheric Stability Schemes

In micrometeorology, six schemes are commonly used to determine the degree of stability or instability. These schemes are Pasquill-Gifford-Turner based on wind speed at 10 m and solar insolation/cloud cover, temperature gradient based on temperature measurements at least two levels, wind speed ratio based on the wind at also two levels, wind direction fluctuation relating with a calculation of standard deviation of horizontal wind direction, gradient Richardson number, bulk Richardson number, and M-O length. For more detail, the description for each scheme can be found in (Golder

1972, Zoumakis 1992, Zoumakis & Kelessis 1993, Mohan & Siddiqui 1998).

Because the wind ratio and the wind direction schemes are directly associated with mechanically generated turbulence as well as temperature gradient scheme is associated more with thermally generated turbulence, their results could not be identified with other results derived from other schemes (Mohan & Siddiqui 1998), which may be attributed to the fact these do not involve ratio scheme of the mechanical-to-convective turbulence. In addition, the Pasquill-Gifford-Turner method requires estimation for parameters such as solar insolation during daytime and an assessment of cloud cover during nighttime. Thus, it cannot be applied in this research. The following subsection describes the methods used in this work to define stability.

Gradient Richardson Number (Ri)

This parameter is the most widely used indicator of atmospheric stability; a nondimensional parameter representing the relative importance of buoyancy and shear in producing turbulence (Kaimal & Finnigan 1994) is

$$\mathrm{Ri} = \frac{\mathrm{g}}{\bar{\mathrm{T}}} \frac{\partial \bar{\theta}/\partial \mathrm{z}}{\left(\partial \bar{\mathrm{u}}/\partial \mathrm{z}\right)^2} \quad \ldots(1)$$

where Θ and u are potential temperature and wind speed at the height z above the ground level, respectively, $\bar{T}$ The mean temperature for the layer and g is the acceleration due to gravity. In this equation $g\,(\partial\bar{\theta}/\partial z)\bar{T}$ is an indicator of convection and $(\partial\bar{u}/\partial z)^2$ is the pointer of mechanical turbulence due to shear force. Ri is positive for stable, negative for unstable, and 0.25 for neutral stratification.

Bulk Richardson number (Rb)

This inductor is a nondimensional stability ratio that uses temperature at two levels but requires wind speed at only one level. It is defined as (Golder 1972):

$$\mathrm{Rb} = \frac{(g/\bar{\theta})\,(\partial\bar{\theta}/\partial z)}{u^2}\,\bar{z}^2 \quad \ldots(2)$$

where $\bar{z}$ Is usually taken to be the geometric mean height $[(z_1{*}z_2)^{1/2}]$.

M-O Stability Parameter $(\bar{z}/L)$

The last key stability parameter is the ratio of $\bar{z}$ to the M-O length (L) (Kaimal and Finnigan, 1994),

$$\frac{\bar{z}}{L} = -\frac{\left(\frac{g}{\bar{\theta}}\right)\left(\overline{w'\theta'}\right)_o}{\frac{u_*^3}{kz}} = \frac{kzg}{\bar{\theta}}\frac{\theta_*}{u_*^2} \quad \ldots(3)$$

where k is the von Kármán constant (=0.4), θ_* is the scaling temperature and u_* is the friction velocity, and $\overline{(w'\theta')}_o$ the mean surface heat flux. In the present paper, the parameters u_* and θ_* are calculated by the following equations (Ashrafi & Hoshyaripour 2010):

$$\mathrm{u}_* = \mathrm{k}\,\Delta\mathrm{u}_\mathrm{z}\left[\ln\frac{\mathrm{z}_2}{\mathrm{z}_1} - \Psi_\mathrm{m}\left(\frac{\bar{\mathrm{z}}}{\mathrm{L}}\right)\right]^{-1} \quad \ldots(4)$$

$$\theta_* = \mathrm{k}\,\Delta\theta_\mathrm{z}\left[\ln\frac{\mathrm{z}_2}{\mathrm{z}_1} - \Psi_\mathrm{h}\left(\frac{\bar{\mathrm{z}}}{\mathrm{L}}\right) + \Psi_\mathrm{h}\left(\frac{\bar{\mathrm{z}}}{\mathrm{L}}\right)\right]^{-1} \quad \ldots(5)$$

The universal function ψ_h under unstable conditions is given by

$$\Psi_\mathrm{m} = 2\ln\left(\frac{1+\mathrm{x}}{2}\right) + \ln\left(\frac{1+\mathrm{x}^2}{2}\right) - 2\tan^{-1}(\mathrm{x}) + \frac{\pi}{2} \quad \ldots(6)$$

with $x = (1 - 16 * \bar{z}/L)^{1/4}$ and for stable conditions is

$$\Psi_\mathrm{m} = -5 * \frac{\bar{\mathrm{z}}}{\mathrm{L}} \quad \ldots(7)$$

In Eq. (5), the function ψ_h for stable conditions is given by

$$\Psi_\mathrm{h} = 2\ln\left(\frac{1+\mathrm{y}}{2}\right) \quad \ldots(8)$$

with $y = (1 - 16 * z/L)^{1/2}$, and lastly, for stable conditions

$$\Psi_\mathrm{h} = \Psi_\mathrm{m} = -5 * \frac{\bar{\mathrm{z}}}{\mathrm{L}} \quad \ldots(9)$$

For the estimation of $\bar{z}/L$ by use of Eq. (3), u_* and θ_* have to be determined from Eqs. (4) and (5) by starting with $\bar{z}/L = 0$ (i.e. $\Psi_h = \Psi_m = 0$). First estimates of u_* and θ_* are then computed, which used to calculate $\bar{z}/L$ by Eq. (3). Subsequently, the new value of $\bar{z}/L$ is substituted in Eqs. (4) and (5) to obtain improved estimates for u_* and θ_*. These steps are repeated for five iteration times to achieve more accuracy for $\bar{z}/L$. The practical advantage of using (4) and (5) is that the large magnitudes of roughness length become unimportant. The limits used to specify stability classes in this study are presented in Table 1.

The Experiment Site and Dataset

Experimental slow response data, including wind speed and air temperature, were used in the presented paper. This experiment occurred at an oil refinery site located in Al-Dura municipality (see Fig. 1), southeast of Baghdad city (33.1° N, 44.2° E, and 40 m above mean sea level). This particular site was chosen because the atmosphere in this site is always pollutant, and it can be considered as a pollution-producing site where in addition to the refinery, a sizable electric power plant is located in the northeast, about 1.5 km distance (Shubbar et al. 2018, Anad et al. 2022). This pollution has several effects on environmental sectors, human health, and local climate behavior (Halos et al. 2017).

For the purpose of the present study, two slow-response meteorological instruments, such as three cup anemometer

Table 1: $\bar{z}/L$, Ri, and Rb limits for stability classification employed in this study.

Type of stability	Symbol	$\bar{z}/L$ interval (Businger 1973)	Ri interval	Rb interval
Extremely unstable	A	$-2.25 < \bar{z}/L < -\infty$	$-1.3 \leq Ri < -\infty$	$Rb < -0.91$
Moderately unstable	B	$-0.11 \leq \bar{z}/L \leq -2.25$	$-0.073 \leq Ri < -1.3$	$-0.91 \leq Rb < -0.051$
Slightly unstable	C	$-0.00023 \leq \bar{z}/L \leq -0.11$	$-0.00017 \leq Ri < -0.073$	$-0.051 \leq Rb \leq -0.00012$
Neutral	D	$\lvert\bar{z}/L\rvert < 0.00023$	$\lvert Ri\rvert < 0.00017$	$\lvert Rb\rvert \leq 0.00012$
Slightly stable	E	$0.23 > \bar{z}/L > 0.00023$	$0.096 \geq Ri > 0.00017$	$0.0672 \geq Rb > 0.00012$
Moderately stable	F	$2.25 > \bar{z}/L > 0.22$	$0.19 \geq Ri > 0.096$	$0.133 \geq Rb > 0.0672$
Extremely stable	G	$\infty \geq \bar{z}/L > 2.25$	$\infty \geq Ri > 0.19$	$Rb > 0.13$

with a vane in one body (Demo-6 type of Chinese origin) and a thermometer, were used. Before running these instruments, the calibration was made with standard instruments used in meteorological offices. The results show that all observations do not appear to have significant differences. The first set is mounted on a tower of 3 m which place on the mid-point of the roof of the water tank (27 m high), so the first height of the instrument location is 30 m, see Fig. 2, which also shows the areas surrounding the experiment site with different directions. About 50 m distance from the first site, the second set was set up on a tower of 15 m.

The observational data: wind speed, its direction, and air temperature measured at two heights were recorded at the same time every 30 seconds for 20 min. It means that the one run length has 40 records of each above parameter. The recording period was 20 days starting from 10 to 20 April 2018, except for two days (18 and 28 days) when the weather was very bad. Every day, the observing runs were taken at different times, from midnight to evening. Briefly, during the whole observing period for both heights, the wind came northwest direction, mostly prevailing. Mean values for air temperature ($\bar{T}$) and wind speed ($\bar{u}$) at two levels with their number runs according to the observing times are presented in Table 2.

In general, at both heights, $\bar{T}$ It has maximum values of 33.6 and 32.2°C, respectively, at noon, while minimum values of 22.4 and 22.1 in the early morning. From $\bar{u}$ Values reported in Table 2, it can be shown that wind speeds at 15 m levels generally are less than those at 30 m levels along all daily times, with a slightly increasing at noon time.

Fig. 1: Photograph of oil Al-Dura refinery.

Fig. 2: Photographs of areas surrounding the site in different directions. The middle photograph shows the location of the measurement instruments.

Table 2: Observing times, number of runs, and mean wind and temperature during this study.

Time	Observing times	No. of runs	$\bar{T}$ (°C)		$\Delta\ \bar{T}$ (°C)	$\Delta\bar{T}/\Delta z$ (°C/m)	$\bar{u}$ (m.s^{-1})		$\Delta\ \bar{u}$ (m.s^{-1})	$\Delta\bar{u}/\Delta z$ s^{-1}
			15 (m)	30 (m)			15 (m)	30 (m)		
	1:00-1:20 am	19	25.1	25.4	0.3	0.02	1.3	4.1	2.8	0.19
Night	1:30-1:50 am	19	24.9	25.1	0.2	0.01	1.5	4.1	2.6	0.17
	2:00-2:20 am	19	24.5	24.7	0.2	0.01	1.2	3.5	2.3	0.15
	2:30-2:50 am	19	24.1	24.5	0.4	0.03	1.6	3.4	1.8	0.12
Early	6:00-6:20 am	17	22.4	22.1	-0.3	-0.02	1.4	3.6	2.2	0.15
morning	7:00-7:20 am	17	23.6	23.3	-0.3	-0.02	1.5	3.6	2.1	0.14
	10:00-10:20 am	19	29.8	28.6	-1.2	-0.08	2.1	4.6	2.5	0.17
Noon	11:00-11:20 am	19	30.7	29.5	-1.2	-0.08	2.3	5.0	2.7	0.18
	2:00-2:20 pm	19	33.1	32.1	-1.0	-0.07	1.8	4.0	2.2	0.15
	3:00-3:20 pm	19	33.6	32.2	-1.4	-0.09	1.9	4.2	2.3	0.15
	5:00-5:20 pm	19	32.6	31.5	-1.1	-0.07	2.2	4.1	1.9	0.13
Afternoon	5:30-5:50 pm	19	31.9	31.1	-0.8	-0.05	2.1	3.9	1.8	0.12
	6:00-6:20 pm	19	31.4	30.8	-0.6	-0.04	1.7	3.6	1.9	0.13
	6:30-6:50 pm	19	30.8	30.3	-0.5	-0.03	1.4	3.3	1.6	0.11
Evening	9:00-9:20 pm	19	27.6	28.4	0.8	0.05	1.6	3.8	2.2	0.15
	10:00-10:20 pm	19	27.0	27.5	0.5	0.03	1.5	3.8	2.3	0.15

RESULTS AND DISCUSSION

Air Temperature Gradient and Wind Shear

Mean vertical temperature gradient $(\Delta\bar{T}/\Delta z)$ between two heights, 15 and 30 m, was calculated for all observing times, and their results are reported in Table 2. From these results, atmospheric lapse rate, i.e., the temperature naturally decreases with elevation, and temperature inversion, i.e., temperature increases with elevation instead of decreasing (Al-Ghrybawi & Al-Jiboori 2020), can be calculated. These quantities play a vital role in determining air stability types and hence, controlling the dispersion of air pollutants (Al-Ghrybawi & Al-Jiboori 2019). Mean lapse rates were dominated at times of the early morning, noon and afternoon, while temperature inversion was at night and evening. The largest lapse rate was found at noon with an average value of -0.08 °C/m and was weak in the early morning and afternoon. In the same way, mean values of temperature inversion in the evening (0.04°C/m) are higher at night (-0.02°C/m).

Wind shear changes wind speed and direction over a short distance (Federal Aviation Administration 2008). It is most often associated with strong temperature inversions. In the last column of Table 2, the mean vertical wind difference (wind shear) through two heights has positive values at all times studied in this paper, which range from 0.11 to 0.19 $s^{-1,}$ and no indication is found.

Diurnal Analysis of Stability

The atmospheric stability has been assessed using gradient Richardson number, bulk Richardson number, and M-O length. The kinds of stability classification using these methods have been determined using the intervals given in Table 1. For detail analysis, the percentage frequency of occurrence of the stability classes for all observation runs at five different times (namely, night, early morning, noon, afternoon, and evening) as well as at two main times of day (i.e., nighttime and daytime) are presented in Figs. 3 and 4, respectively. Generally, results from Ri and Rb schemes are primarily closed, especially in classes B and C.

During the nighttime, frequencies for stability classes from E to G are larger than others, while during the noon and afternoon times (see Fig. 3c and 3d), frequencies for classes

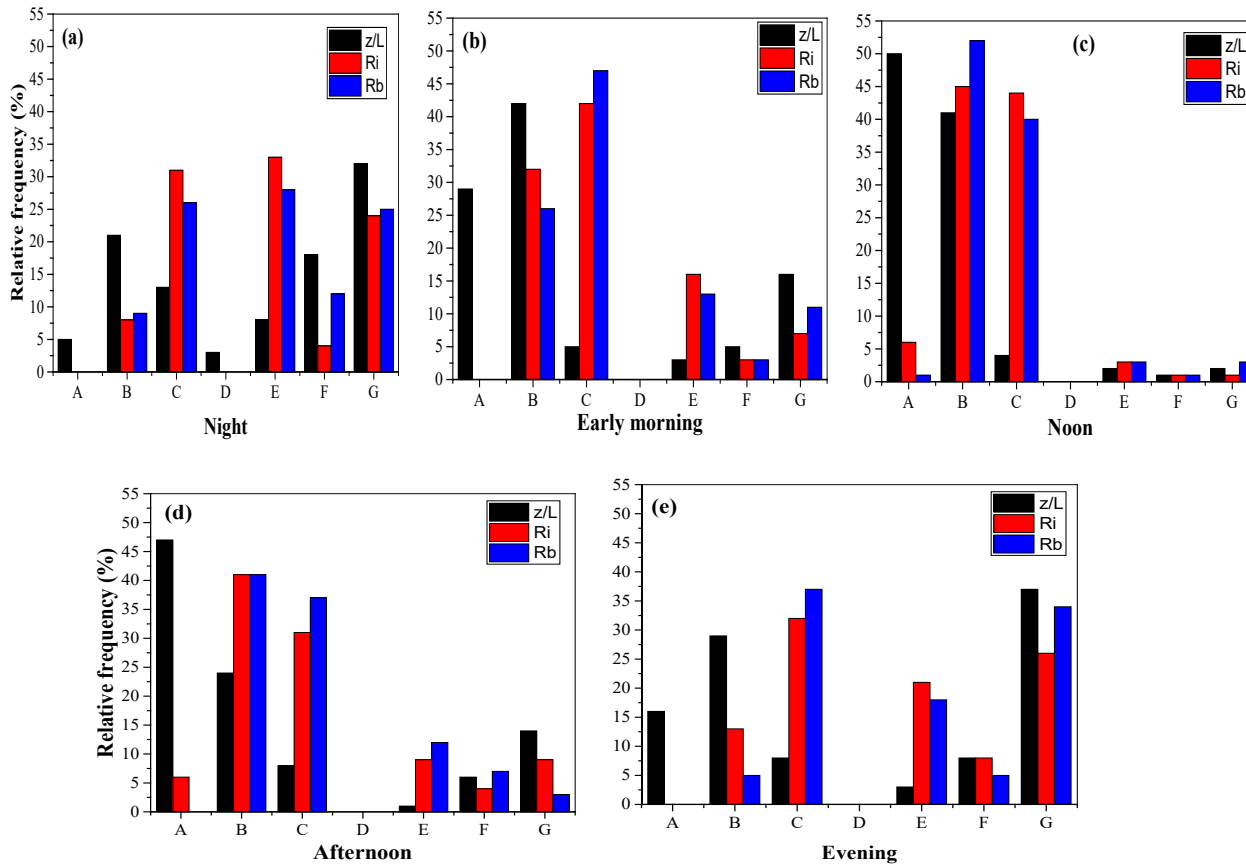

Fig. 3: Percentage of frequencies of occurrence of stability classes using $\bar{z}/L$, Ri and Rb for times (a), (b), (c), (d), and (e).

B and C are the largest. Class B is the most frequent in the early morning, and in the evening, there is a large variation in the frequency distribution.

Now results for stability classes calculated in the presented paper at five times above are unified into two primary times of the whole day, i.e., nighttime (night and evening) and daytime (early morning, noon, and afternoon), as shown in Figs. 4a and 4b, respectively.

Hourly evaluation of results reveals that instability increases from sunrise to local noon and decreases from noon to sunset, while variation in stability is vice versa. During the daytime, most frequencies in classes B and C obtaining from Ri and Rb schemes, while class A derived from $\bar{z}/L$, is the largest. In contrast, at nighttime, most frequencies are of class G, derived from $\bar{z}/L$, scheme and of classes F and G obtained from Ri and Rb.

Fig. 5 shows the comparison among the results obtained from three classification schemes by calculating the percentage of relative frequencies of occurrences of the stability classes for each stability class. Generally, all schemes show a wide variation of stability between in- and stability. The stability classes show a good agreement for the results obtained from schemes Ri and Rb. As shown in this figure, instability cases are frequent, especially for B- and C-class, while stability cases are less. As expected, neutral class D has no results, just only a few frequencies for z/L, because it is rare in the real atmosphere (Arya 2001, Al-Jiboori 2010). Class B, D, F, and G frequencies are often closed. Still, they have significant differences in classes A and C, especially M-O length, as illustrated in Fig. 5. This difference is expected because the application of the M-O scheme needs exact information such as those measured by fast-response instruments.

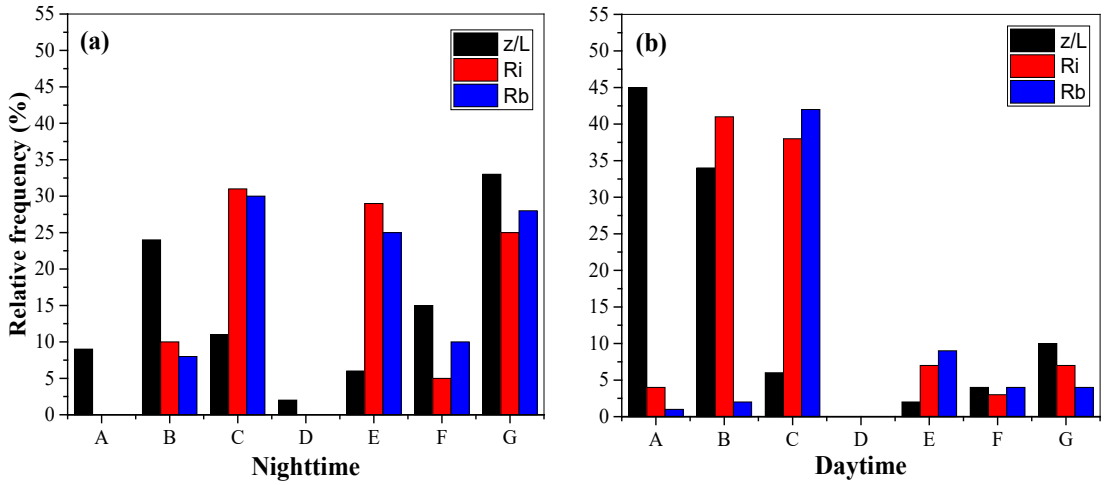

Fig. 4: Percentage of relative frequencies of occurrence of stability classes derived from $\bar{z}/L$, Ri and Rb for two times (a) nighttime and (b) daytime.

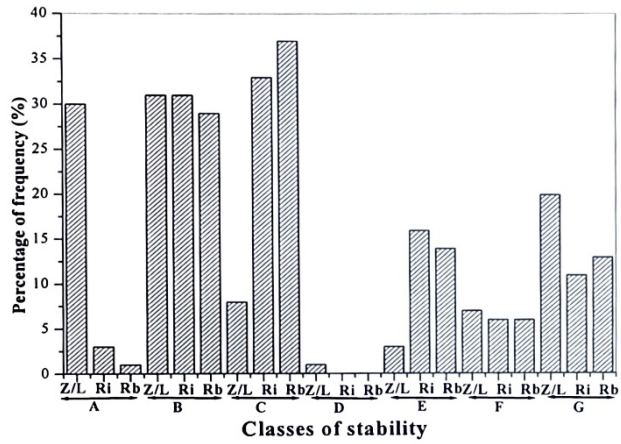

Fig. 5: Percentage of availability of atmospheric stability classes obtained by $\bar{z}/L$, Ri and Rb schemes.

CONCLUSIONS

Based on the observational measurements of wind speed and air temperature at two levels, 15 and 30 m, which came from the field experiment at the Dura refinery, southeast of Baghdad, atmospheric stability has been estimated from three different schemes. Stability classes and their frequency of occurrence were obtained. Results showed that the majority of stable to very stable atmospheric conditions and periods of temperature inversions occur in the evening and night. During the day, between 6 am and 7 pm, atmospheric stability tends to be most unstable, with a few neutral conditions and even fewer stable or inversion conditions.

The relevance of instability during the day and stability at night was obtained from the schemes: z/L, Ri, and Rb with relative frequencies of 85%, 83%, and 83% and 54%, 60%, and 63%, respectively. During the day, instability increases from sunrise to local noon and decreases from noon to sunset, while variation in stability is vice versa.

ACKNOWLEDGMENT

The authors of the present work express their deepest appreciation to Mustansiriyah University (www.uomustansiriyah.edu.iq) for their support during the work.

REFERENCES

Al-Ghrybawi, A.R. and Al-Jiboori, M.H. 2019. Study of surface heat inversions characteristics around Baghdad station. Sci. Rev. Eng. Environ. Sci., 28(4): 610-618. doi:10.22630/PNIKS.2019.28.4.55

Al-Ghrybawi, S.R. and Al-Jiboori, M.H. 2020. Study of Intensity and thickness of surface heat inversion for Baghdad. J. Phys. Conf. Ser.,9: 1660. doi:10.1088/1742-6596/1660/1/012072

Al-Jiboori, M.H. 2010. Determining neutral and unstable wind profiles over Baghdad city. Iraqi J. Sci., 51(2): 343-350.

Al-Jiboori, M.H., Yumao, X. and Yongfu, Q. 2001. Effects of different terrain on velocity standard deviations. Atmos. Sci. Lett., 11: 1-7. doi:10.1006/asle.2001.0038

Anad, A.M., Hassoon, A.F. and Al-Jiboori, M.H. 2022. Assessment of air pollution around Durra refinery (Baghdad) from emission NO2 gas at April Month. Bagh. Sci. J., 19: 515-522. doi:http://ds.doi.org: 10.21123/bsj.2022.19.3.0515

Anto, A.F., Hasse, L. and Murty, C.S. 1980. Stability parameters and their inter-relationships at the Naviface. Mahasagar Bull. Natl. Instit. Oceanogr., 13(4): 295-301.

Arya, S.P. 2001. Introduction to Micrometeorology. Second edition. Academic Press, San Diego, USA.

Ashrafi, K. and Hoshyaripour, A. 2010. A model to determine atmospheric stability and correction with CO concentration. Int. J. Environ. Sci. Eng., 2: 83-88.

Businger, J.A. 1973. Turbulent Transfer in the Atmospheric Surface Layer. American Meteorology Society, CA.

Federal Aviation Administration. 2008. Wind Shear. Retrieved from http://FAASafety.gov

Golder, D. 1972. Relation among stability parameters in the surface layer. Bound. Layer Meteorol., 13: 47-58.

Halos, S.H., Al-Taai, U.T. and Al-Jiboori, M.H. 2017. Impact of dust events on aerosol optical properties over Iraq. Arab. J. Gesci., 10: 263. doi:10.1007/s12517-017-3020-2

Kaimal, J.C. and Finnigan, J.T. 1994. Atmospheric Boundary Layer Flows: Their Structure and Measurement. Oxford University Press, Oxford, UK

Lazaridis, M. 2011. First Principles of Meteorology Air Pollution. Springer, Cham. doi:10.1007/978-94-007-0162-5

Mohan, M. and Siddiqui, T.A. 1998. Analysis of various schemes for the estimation of atmospheric classification. Atmos. Environ., 32: 3775-3781.

Newman, J.F. and Klein, P.M. 2014. The impacts of atmospheric stability on the accuracy of wind speed extrapolation methods. Resources, 3: 81-105. doi:10.3390/resources.3010081

Rodrigo, J.S., Cantero, E., Garcia, B., Borbon, F., Irigoyen, U., Lozano, S., Fernandes, P.M. and Chavez, R.A. 2015. Atmospheric stability assessment for the characterisation of offshore conditions. J. Phys. Conf. Ser., 625: 1-11. doi:1.1088/1742-6596/625/1/012044

Seinfeld, J.H. and Pandis, S.N. 1998. Atmospheric Chemistry and Physics: From Air Pollution to Climate Change (Vol. 51). John Wiley & Sons. Inc., NJ.

Shubbar, R.S., Suadi, A.J. and Al-Jiboori, M.H. 2018. Study the concentration of SO2 emitted from Daura refinery by using a screen view model. Al-Mustansiriyah J. Sci., 29(3): 7-15. doi:http://doi.org/10.23851/mjs.v29i3.616

Zoumakis, N.M. 1992. On the relationship between the gradient and bulk Richardson number for the atmospheric boundary layer. Nuovo cimento, C15: 111-116.

Zoumakis, N.M. and Kelessis, A.G. 1993. On the theoretical relationship between the Monin-Obukhov stability parameter and the bulk Richardson number. Nuovo cimento, 16C, pp. 1-6.